Supplement of Atmos. Chem. Phys., 15, 3217–3239, 2015
http://www.atmos-chem-phys.net/15/3217/2015/
doi:10.5194/acp-15-3217-2015-supplement

Atmospheric Chemistry and Physics
Open Access

Supplement of

Seasonal changes in the tropospheric carbon monoxide profile over the remote Southern Hemisphere evaluated using multi-model simulations and aircraft observations

J. A. Fisher et al.

Correspondence to: J. A. Fisher (jennyf@uow.edu.au)

S1 Construction of observationally-derived metrics

In Tables 5 and 6 in the main text, we tabulate a set of metrics, based on the Cape Grim Overflight Program (CGOP) observations, than can be used to quickly diagnose the performance of atmospheric chemistry models in the SH remote free troposphere. Here, we provide details of the fitting methodologies so that they can be easily applied to future model revisions.

S1.1 Seasonal cycles

We describe the average CO seasonal cycles in three altitude bins using a harmonic fit to the observations, similar to Pak et al. (1996) and Francey et al. (1999). We assume no trend in the data exists over the 9-year observation period and therefore fit a mean annual cycle. We assumed the observations could be represented by a harmonic function of the form

$$X(t) = \sum_i [a_i \sin(2\pi i t) + b_i \cos(2\pi i t)] + C \qquad \text{(S1)}$$

where the sum is over the number of harmonic terms (i), t is the time in fractional year, C is a constant that represents the overall mean CO mixing ratio in each altitude bin, and a_i and b_i are constants that combined describe the amplitude and phase of each harmonic term.

We divided the observations into three altitude bins (0-2, 2-5, and 5-8 km as in Fig. 3) and computed the median for each year/month to create a time series of monthly median values. We performed least squares fits of Eqn. S1 assuming existence of between one and four harmonic terms. In all cases, we found that only the first harmonic term was statistically significant at the p=0.05 level or better, so only the results from the first order harmonic were retained. Below 2 km, the single harmonic fit maximised the adjusted r^2. Above 2 km there was a marginal improvement to the adjust r^2 when the second harmonic was included, but because the improvement was so small and the additional terms were not significant we do not include them here. The amplitude (A) and phase (φ) were calculated from the fit coefficients a and b using standard trigonometric relationships ($A = \sqrt{a^2 + b^2}$; $\varphi = atan2(b, a)$). From the amplitude and phase shown in Table 5, the first-order harmonic fit to the observations can be reconstructed as

$$X(t) = A \sin(2\pi(t + \varphi)) + C \qquad \text{(S2).}$$

The reconstructed time series are shown along with the original observations in Fig. S5. The fit coefficients are given in Table 5 for the observations and in Table S2 for the models.

S1.2 Vertical profiles

We describe the average CO vertical profile in each season using a polynomial fit to the median 1-km binned observations. We assumed the median profiles could be represented by a polynomial function of the form

$$X(z) = \sum_i a_i z^i \qquad \text{(S3)}$$

where the sum is over the number of polynomial terms (i), z is the altitude in kilometers, and the a_i are the fit coefficients.

We divided the observations into four seasons (DJF, MAMJ, JA, and SON as in Fig. 4), grouped into 1-km bins, and computed the median vertical profile for each season. We performed least squares fits of Eqn. S3 assuming existence of between one and four polynomial terms. The number of polynomial terms included in the final fit for each season was chosen minimize the residual error and maximize the adjusted r^2. All final fits were significant at the p=0.01 level or better. From the fit coefficients shown in Table 6, the fit to each vertical profile can be recreated using Eqn. S3. The reconstructed profiles are shown along with the original observations in Fig. S6. The fit coefficients are given in Table 6 for the observations and in Table S3 for the models.

Tables

Table S1. Long-term trends in surface CO at Cape Grim. [a]

Time Period	Season	Trend [b]		p-value
		ppbv yr^{-1}	% yr^{-1}	
1991-2008 (CGOP, SHMIP)	**DJF**	-0.12 (-0.38, +0.20)	-0.25 (-0.75, +0.47)	0.60
	MAMJ	-0.01 (-0.21, +0.21)	-0.02 (-0.42, +0.47)	0.97
	JA	-0.11 (-0.31, +0.07)	-0.18 (-0.50, +0.13)	0.24
	SON	-0.17 (-0.38, +0.06)	-0.26 (-0.56, +0.10)	0.11
	Annual	-0.02 (-0.22, +0.21)	-0.04 (-0.40, +0.41)	0.81
1991-2011 (CGOP, SHMIP, HIPPO)	**DJF**	-0.12 (-0.37, +0.12)	-0.25 (-0.74, +0.26)	0.39
	MAMJ	-0.07 (-0.22, +0.08)	-0.15 (-0.45, +0.17)	0.34
	JA	-0.10 (-0.26, +0.11)	-0.18 (-0.43, +0.18)	0.26
	SON	-0.21 (-0.38, -0.01)	-0.31 (-0.56, -0.02)	0.03
	Annual	-0.07 (-0.25, +0.10)	-0.14 (-0.44, +0.20)	0.41
2004-2011 (SHMIP, HIPPO)	**DJF**	+0.11 (-0.80, +1.13)	+0.26 (-1.67, +2.77)	0.61
	MAMJ	+0.14 (-0.58, +1.01)	+0.32 (-1.19, +2.44)	0.69
	JA	+0.32 (-0.63, +1.22)	+0.56 (-1.07, +2.32)	0.59
	SON	-0.56 (-1.46, +0.11)	-0.88 (-2,19, +0.17)	0.11
	Annual	-0.24 (-0.53, +1.04)	+0.48 (-0.96, +2.25)	0.54

[a] Surface CO measurements are from CSIRO flask samples collected at the Cape Grim Baseline Air Pollution Station. Trend estimates use the Theil-Sen method (Sen, 1968) as implemented in the R *openair* package (Carslaw & Ropkins, 2012).
[b] Numbers in parentheses give the 95% confidence intervals for the estimated trend.

Table S2. Same as Table 5, but for the four SHMIP models. Bold values indicate the simulated coefficients are within the 95% confidence interval of those from the CGOP observations.

Altitude Range	Model	Constant (ppbv)	Amplitude (ppbv)	Phase (years)
0-2 km	GEOS-Chem	57.0	9.4	-0.392
	NIWA-UKCA	**53.5**	**10.1**	-0.414
	TM5	64.7	**10.3**	-0.396
	CAM-chem	46.6	9.0	-0.429
2-5 km	GEOS-Chem	**60.4**	**10.8**	**-0.397**
	NIWA-UKCA	**58.5**	**11.5**	-0.423
	TM5	72.6	**11.3**	-0.422
	CAM-chem	49.8	**10.9**	**-0.412**
5-8 km	GEOS-Chem	**63.6**	**13.7**	**-0.408**
	NIWA-UKCA	**63.2**	**13.6**	-0.432
	TM5	77.6	**13.3**	-0.446
	CAM-chem	54.1	**12.5**	-0.430

Table S3. Same as Table 6, but for the four SHMIP models. Bold values indicate the simulated coefficients are within the 95% confidence interval of those from the CGOP observations.

Season	Model	a_0	a_1	a_2	a_3	a_4
DJF	GEOS-Chem	46.6	**1.3**	0.047	-0.010	--
	NIWA-UKCA	**45.2**	**2.2**	-0.10	-0.00028	--
	TM5	53.3	4.6	-0.60	0.04	--
	CAM-chem	**42.4**	**-2.4**	**0.80**	**-0.050**	--
MAMJ	GEOS-Chem	51.3	**1.4**	**-0.019**	**-0.011**	--
	NIWA-UKCA	**45.9**	**1.4**	**0.14**	**-0.017**	--
	TM5	56.8	4.5	-0.63	0.041	--
	CAM-chem	40.2	**0.93**	**0.09**	**-0.0097**	--
JA	GEOS-Chem	**60.4**	**2.4**	**-0.10**	--	--
	NIWA-UKCA	**57.7**	**2.3**	**-0.04**	--	--
	TM5	68.4	**3.5**	**-0.20**	--	--
	CAM-chem	47.6	**3.2**	**-0.20**	--	--
SON	GEOS-Chem	**64.1**	**-2.4**	**2.2**	-0.34	0.016
	NIWA-UKCA	**63.3**	**-1.3**	**1.8**	-0.30	0.016
	TM5	69.7	**4.7**	**-0.73**	**0.16**	**-0.012**
	CAM-chem	**57.2**	**-4.7**	**3.0**	-0.48	0.026

Figures

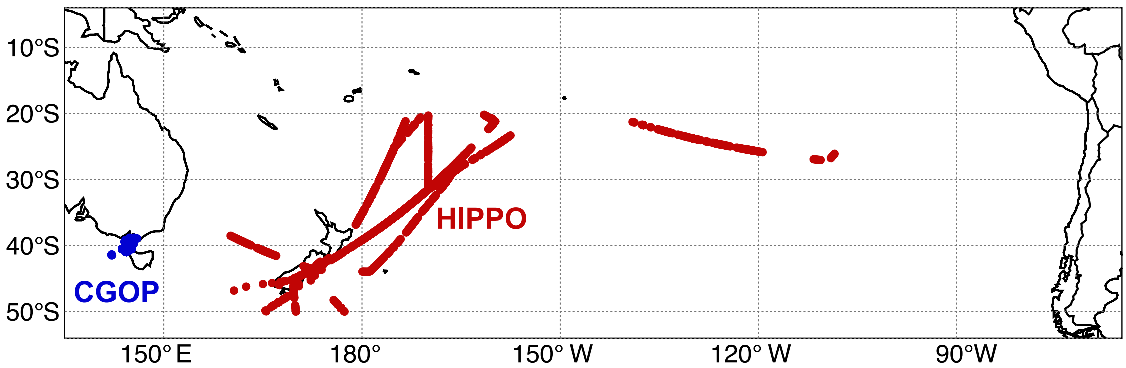

Figure S1. Sampling locations for CGOP (blue) and HIPPO (red) used in this work. CGOP includes all flask samples except those located near Melbourne. HIPPO includes merged observations below 8 km over South Pacific mid-latitudes (20-50°S, 160°E-90°W) for which "best available" CO measurements exist (see text). HIPPO data collected at low altitudes over the city of Christchurch are excluded from the analysis.

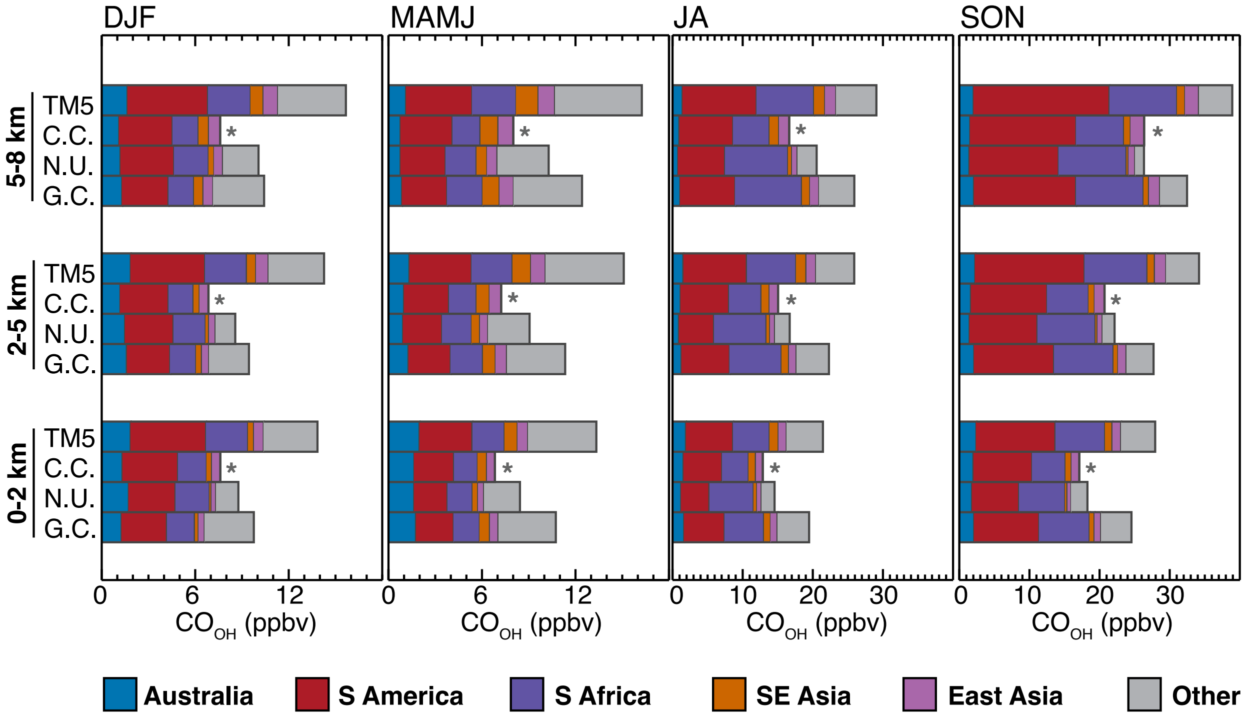

Figure S2. Same as Fig. 7 but for CO_{OH}. The * indicates the "other" contribution could not be calculated in CAM-chem as the simulation did not include a global CO_{OH} tracer.

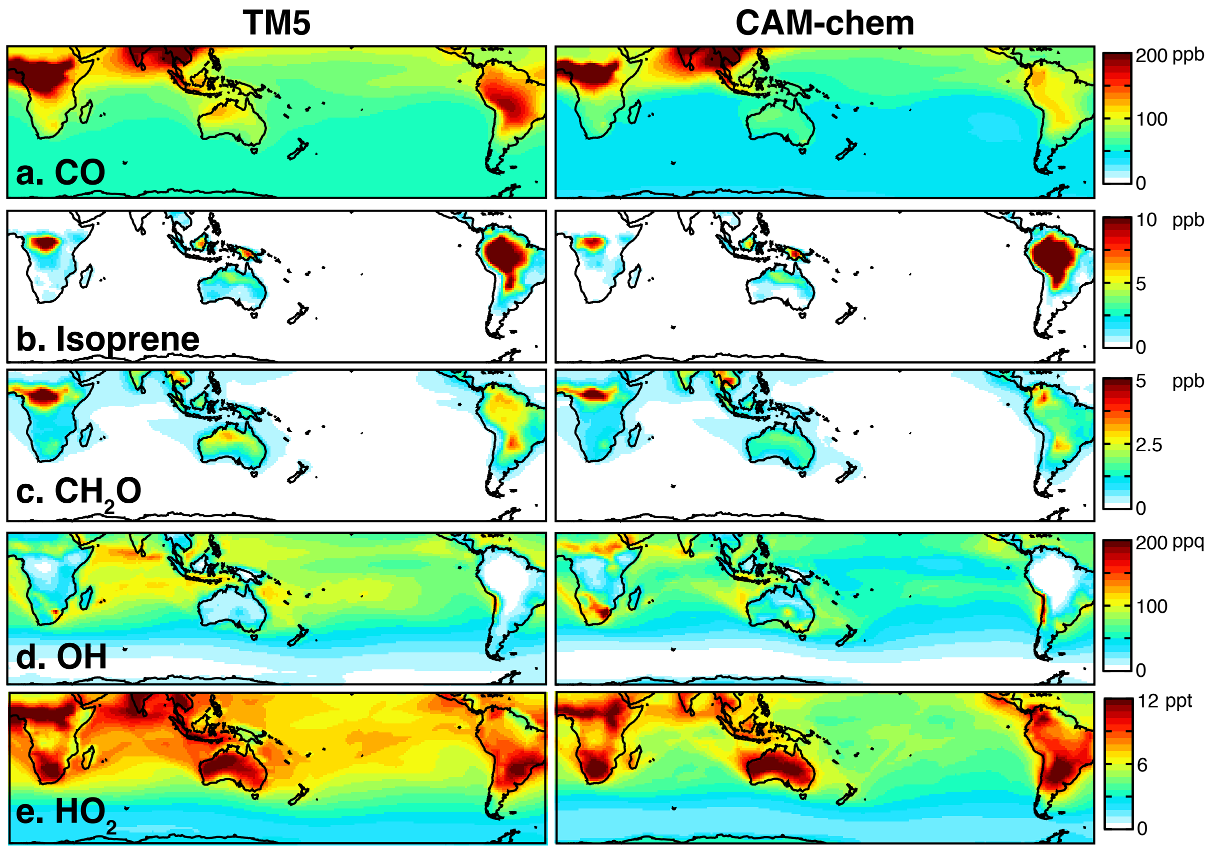

Figure S3. Same as Fig. 8, but for TM5 and CAM-chem.

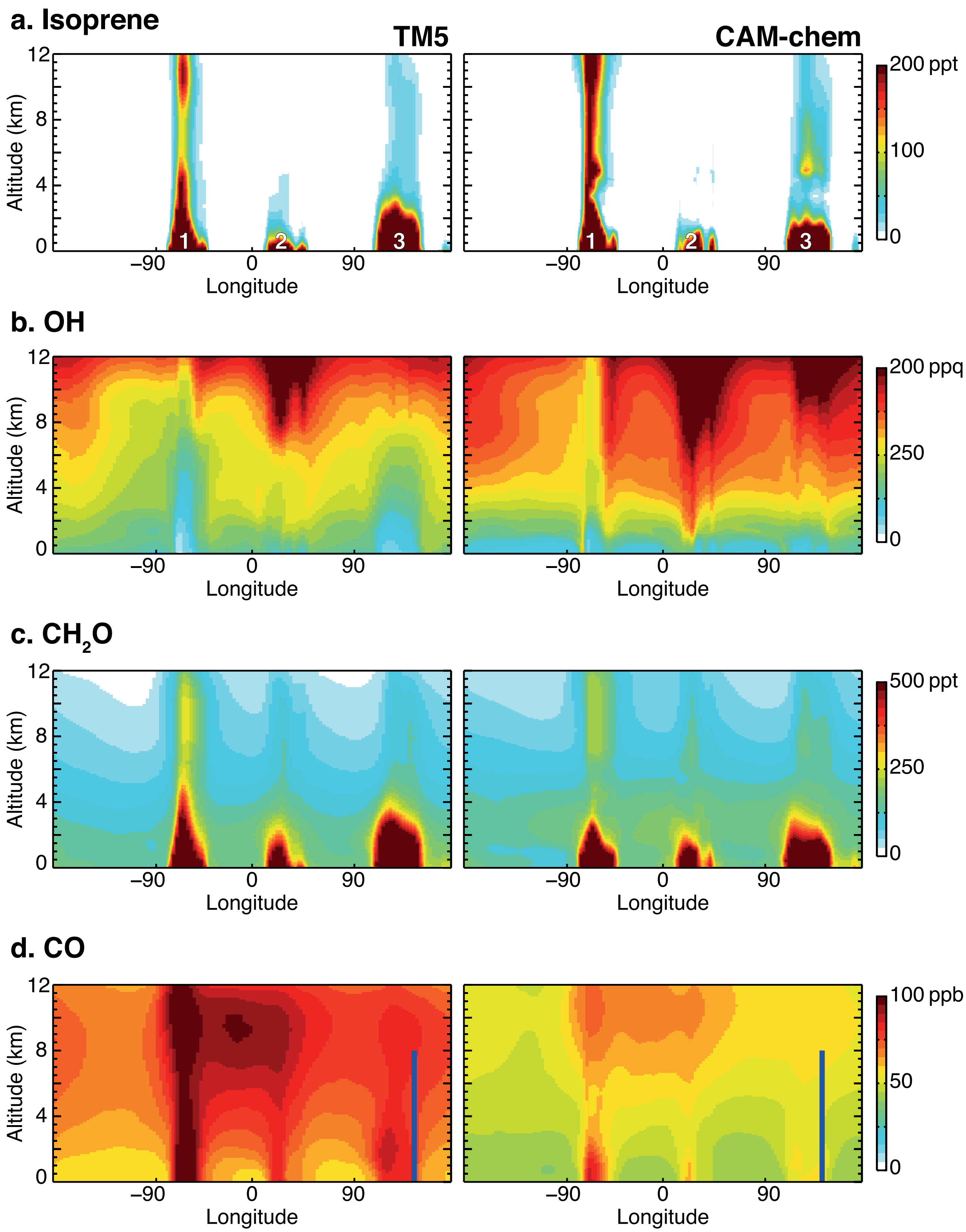

Figure S4. Same as Fig. 9, but for TM5 and CAM-chem.

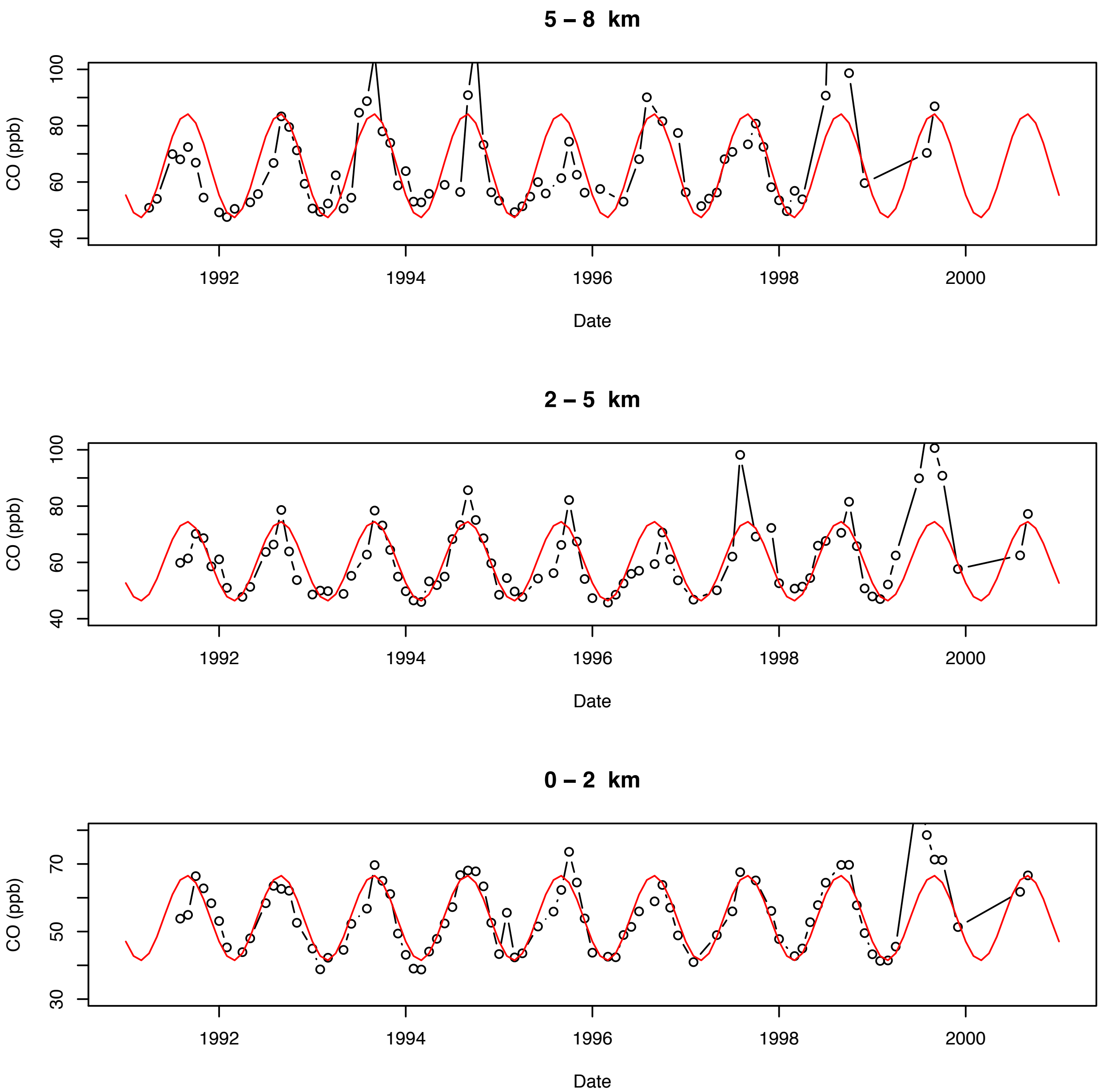

Figure S5. Time series of CO observations from CGOP in three altitude bins (black), along with the reconstructed time series computed using the first harmonic term in each altitude bin as given in Table 5 (red).

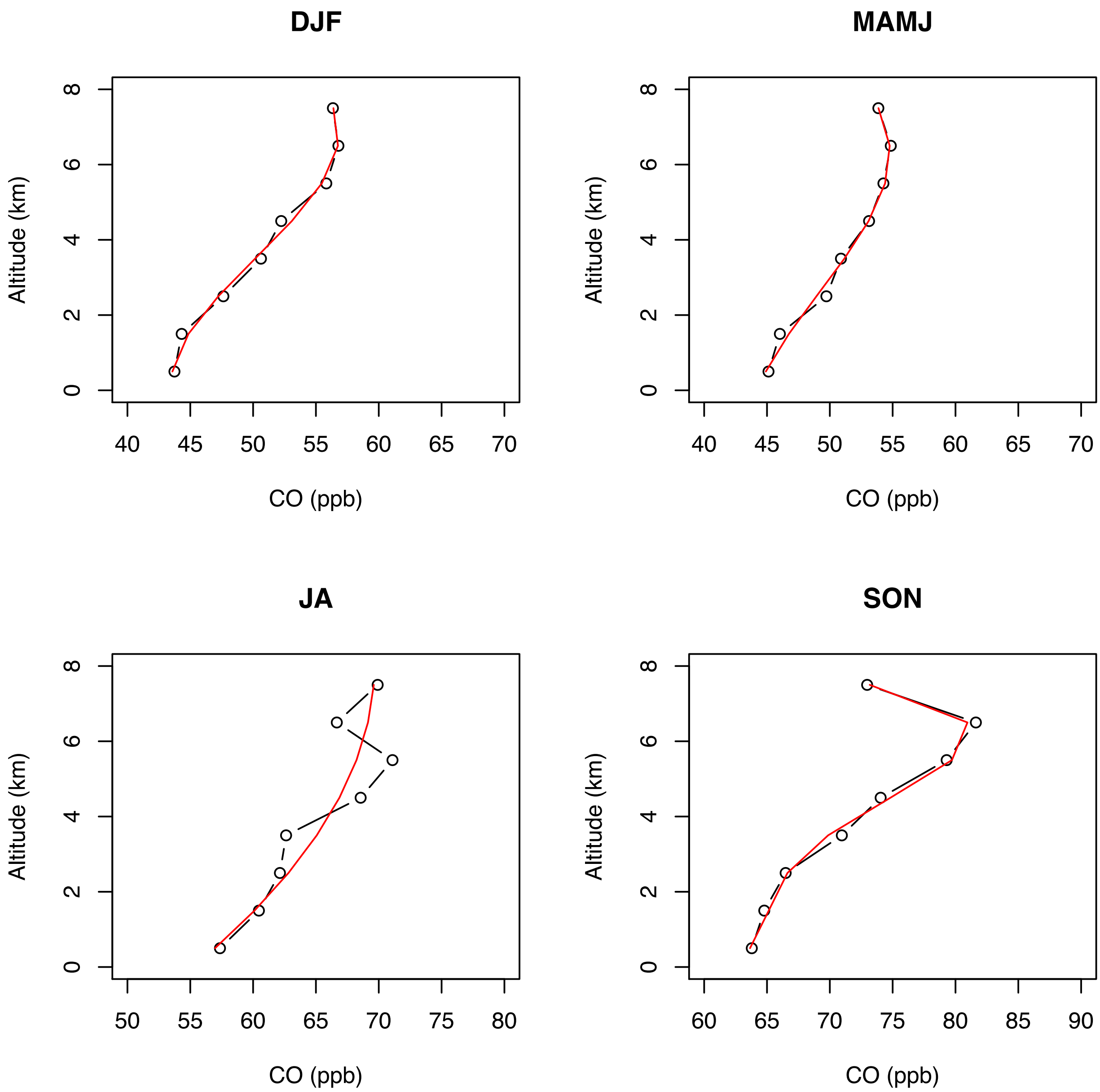

Figure S6. Median CO vertical profiles from CGOP in each season (black), along with the reconstructed profile computed using the polynomial terms in each altitude bin as given in Table 6 (red).

References

Carslaw, D. C. and Ropkins, K.: openair – An R package for air quality data analysis, Environ. Modell. Softw., 27-28, 52-61, doi:10.1016/j.envsoft.2011.09.008, 2012.

Francey, R., Steele, L., Langenfelds, R., and Pak, B.: High precision long-term monitoring of radiatively-active trace gases at surface sites and from ships and aircraft in the Southern Hemisphere atmosphere, J. Atmos. Sci., 56, 279–285, 1999.

Pak, B., Langenfelds, R., Francey, R., Steele, L., and Simmonds, I.: A Climatology of Trace Gases from the Cape Grim Overflights, 1992–1995, Baseline Atmospheric Program (Australia) 1994–1995, Bureau of Meteorology and CSIRO Division of Atmospheric Research, Melbourne, Victoria, Australia, 41–52, 1996.

Sen, P. K.: Estimates of the Regression Coefficient Based on Kendall's Tau, J. Am. Stat. Assoc., 63 (324), 1379-1389, 1968.